

Determination of 2D Quasi Incompressible Flow around a Recorder Labium: a Comparison between Different Methods

R. Auvray, B. Fabre

LAM - D'Alembert,
UPMC Univ Paris 06, UMR CNRS 7190,
11 rue de Lourmel, 75015 Paris, France
auvray@lam.jussieu.fr
benoit.fabre@upmc.fr

P.-Y. Lagr e

CNRS, D'Alembert,
UPMC Univ Paris 06, UMR CNRS 7190,
4 place Jussieu, 75005 Paris, France
pierre-yves.lagree@upmc.fr

ABSTRACT

The shape of the labium has important consequences on the sound produced by flute-like instrument. This statement is well known by instrument makers who take extremely care with this precise part. The sharp edge of the labium modifies both acoustic and hydrodynamic properties. Non-linear acoustic phenomena and intricate vortex structures might strongly depend on the shape of the labium. A first step in the study of the labium is to consider the acoustic part only. This paper presents a comparison of different numerical methods to estimate the linear part of the acoustic flow around the labium. Results are discussed with respect to the sharpness and the angle of the labium, two main features of the labium that have already been studied experimentally. Finally, one of the methods is proposed as a good candidate to include in a sound production model.

1. INTRODUCTION

In flue instruments a planar air jet is blow towards a sharp edge called the labium. The shape of the labium is known by instrument makers to be crucial in timbre and attack response of flute-like instruments. Whether it is a recorder, a flute or an organ flue pipe, the sound properties of such instruments are not intended to be the same, and so are their labium shapes.

From a physical point of view, the presence of a relatively sharp edge within the resonator and also within the jet flow will have consequences on the acoustics and the aeroacoustics of the instrument, respectively.

The constriction of the window and the sharp edge affect the acoustic transverse flow around the labium. Intuitively, the acoustic velocity is expected to be accelerated while approaching the labium. For high amplitude of oscillation, the flow separation may occur at the labium [1]. The mechanisms of vorticity generation at the labium have been modeled by Howe [2], and identified as strong acoustic damping mechanisms by Howe [3] and Fabre *et al.* [4]. The sharpness and the angle of the labium are associated

with the generation of vorticity, and thus have a great influence on this damping mechanism.

Conversely to the generation of vorticity at the labium, the generation and modulation of the vorticity of the jet within the window is often discussed as the core of sound production modeling. Based on works of Howe [2] and Nelson *et al.* [5], Dequand *et al.* [6] proposed a *discrete-vortex* model in which sound production is ensured by the interaction of propagating discrete vortices with the acoustic flow. According to this model, the source mechanisms depend on the orientation of the acoustic flow near the labium and might be modified by a change in the labium geometry.

Experimental observations of Dequand *et al.* [6] confirm the influence of the labium angle on the sound spectra. A further validation of the *discrete-vortex* model would be to include in the model the labium geometry influence through the modification of the acoustic streamlines and to check the resulting sound spectra. A first step is to develop a consistent description of the acoustic flow within the window. This is the aim of the present study.

Four different methods to estimate the flow acoustic around the labium are presented in section 2 and compared in section 3. The effect of two main characteristics of the labium, the sharpness and the angle, are then presented in section 4. Results are discussed in section 5.

2. PRESENTATION OF THE METHODS

In an aeroacoustical analysis of sound production in such instruments, where a jet interacts with an acoustic resonator, the exact definition of the acoustic flow is one of the key points. Following Howe [2], the acoustic flow is here defined as the fluctuating part of the potential component of the total flow.

This section presents four methods to study such a potential flow. Three of them are based on the assumption that the flow within the window is incompressible since the length of the window W is much smaller than the acoustic wavelength. This is therefore a low frequency approximation. In this case, the two components of the flow are denoted u and v . In the last method, the compressibility is taken into account and the two components of the flow are then denoted u' and v' .

The two first methods (complex potential and Schwarz-

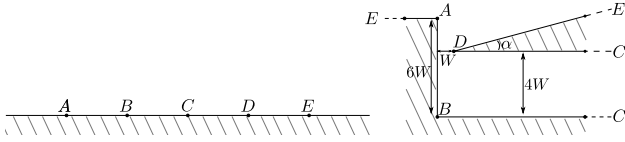


Figure 1. Transformation of the upper half plan (left) to the recorder window geometry (right) with the Schwarz-Christoffel transformation.

Christoffel transformation) are usual methods of fluid mechanics. It can be shown that they are equivalent for simple cases, even if the second can be used for more intricate geometry. The first actually corresponds to the theoretical study of a flow around an angle. The two last methods use the Finite Element Method (FEM) to solve either an incompressible or a compressible flow equation.

2.1 Incompressible flow around an angle: complex potential

For an incompressible potential flow, the velocity satisfies the two relations:

$$\nabla \cdot \mathbf{u} = 0 \quad \text{and} \quad \nabla \times \mathbf{u} = 0. \quad (1)$$

A description of the two-dimensional flow is possible thanks to the potential ϕ and the streamfunction ψ defined as

$$\begin{cases} u = \frac{\partial \phi}{\partial x} = \frac{\partial \psi}{\partial y} \\ v = \frac{\partial \phi}{\partial y} = -\frac{\partial \psi}{\partial x} \end{cases}, \quad (2)$$

that automatically satisfy the condition in Eq. (1). The study of the flow can be reduced to the complex analysis of the complex potential f defined as:

$$f = \phi + i\psi. \quad (3)$$

The complex velocity $w = u - iv$ is then given by

$$w = \frac{df}{dz}. \quad (4)$$

The complex analysis of the singularities of f yields to well known flows. Among others, the case [7]

$$f = z^n \quad (5)$$

has been identified as the flow around an angle $\alpha = \pi(2 - 1/n)$. The characteristics of the flow are:

$$\begin{cases} \phi = r^n \cos n\theta \\ \psi = r^n \sin n\theta \end{cases} \quad \text{or} \quad \begin{cases} u = nr^{n-1} \cos(n-1)\theta \\ v = -nr^{n-1} \sin(n-1)\theta \end{cases}, \quad (6)$$

where r and θ are the cylindrical coordinates in a referential where the tip of the angle is at $r = 0$. Note that for angles α smaller than π the velocity diverges while approaching the tip of the angle.

2.2 Incompressible flow through the recorder window: Schwarz-Christoffel transformation

Another way to obtain a two dimensional flow in a given geometry under potential assumptions is to use the Schwarz-Christoffel transformation of the upper half complex plane

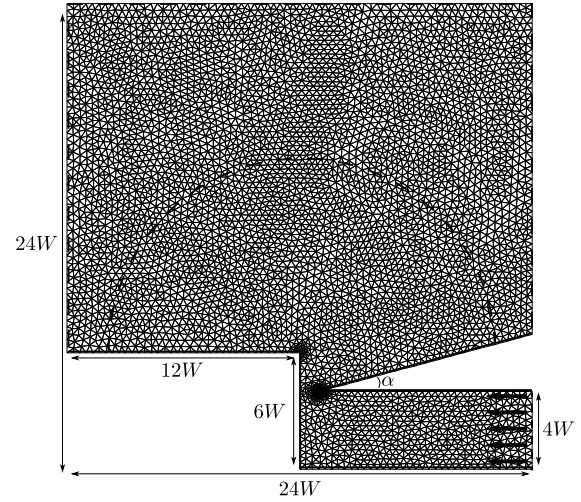


Figure 2. Domain of computation for the Finite Element Method. Solid lines are walls. Outer dashed line are outflow boundary. The half circle in dashed line represents the beginning of the PML condition for the compressible case. The lower dashed line is the inflow condition. The mesh generated by the software *FreeFem++* is refined near the tip of the labium with an adaptive algorithm whose error criteria is based on the modulus of the velocity.

into a given geometry. The transformation used in this paper is illustrated on figure 1. The computation of the transformation is made thanks to the numerical toolbox developed by Driscoll [8]. The conformal mapping allows to obtain the streamlines at any required position, i.e. it allows to obtain the streamfunction ψ and the velocity \mathbf{u} .

This method has already been applied to study jet receptivity in a recorder [9] and *discrete-vortex* model [6], although it was used in a ideal case with an infinite plate as the labium and no wall facing it.

2.3 Incompressible flow through the recorder window: FEM

It is also possible to solve the flow around the labium by direct numerical computation. The incompressibility equation $\nabla \cdot \mathbf{u} = 0$ is rewritten:

$$\Delta \psi = 0, \quad (7)$$

where Δ is the Laplacian operator and ψ the streamfunction defined in Eq. (2). This equation is solved with the Finite Element Method (FEM) whose only difficulties lie in handling the mesh and the boundary conditions. The domain of computation is shown on figure 2. The constant velocity u_0 on the inflow boundary yields to the condition:

$$\psi = u_0 y. \quad (8)$$

The normal velocity on the wall is zero, which leads to the condition:

$$\begin{cases} \psi = 0 & \text{for the bottom} \\ \psi = 4W u_0 & \text{for the labium} \end{cases}, \quad (9)$$

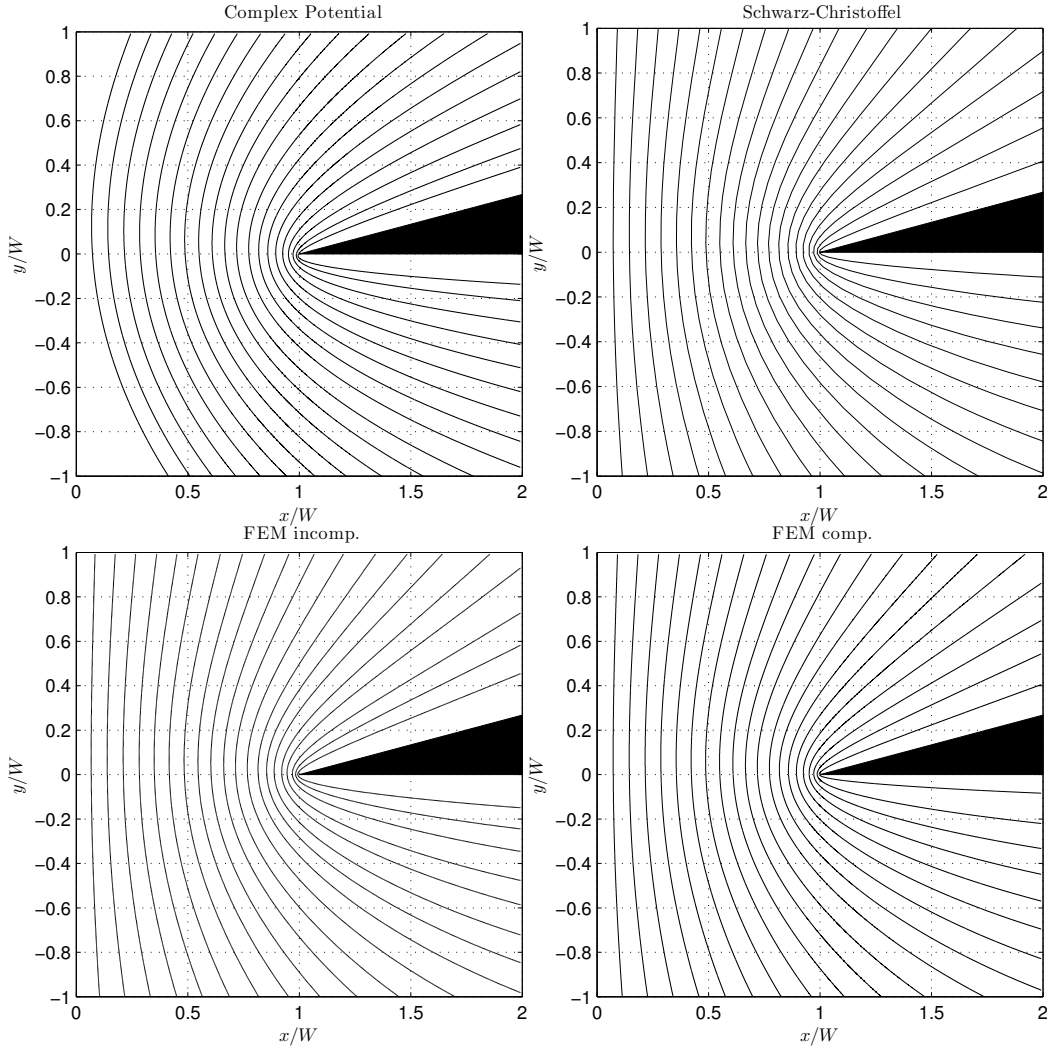


Figure 3. Streamlines computed with the different methods. Except for the complex potential method, the vertical wall stands at $x = 0$ and the bottom wall at $y = -4W$). The Mach number for the FEM computation is $M \approx 10^{-4}$. The Helmholtz number of the compressible FEM computation is $He = 0.004$.

accordingly to the inflow condition (see Eq. (8)). The outflow condition is handled as follow:

$$\psi = u_0 4W \frac{\theta_r - \pi}{\theta_0 - \pi} \quad (10)$$

where the angle $\theta_r = \tan^{-1}((y-y_0)/(x-x_0))$ is the angle of the coordinate on the boundary with respect to the center $(x_0, y_0) = (W, 0)$. This corresponds to the incompressible outflow of a source ($f(z) = \log(z)$), located at the tip of the labium. The mesh is generated by the same software used to solve the FEM: *FreeFem++* [10]. The mesh is automatically refined near the region of interest –as shown on figure 2– with an adaptive algorithm [11] whose error criteria is based on the modulus of the velocity.

2.4 Compressible flow through the recorder window: FEM

Even if the incompressible assumption is widely justified since the window W is much smaller than the wavelength at low frequencies, it is worth computing the compressible flow around the labium. Besides, the FEM requires no

more computation cost than for the incompressible case.

The Helmholtz equation on the pressure p

$$\Delta p + k^2 p = 0 \quad (11)$$

is solved for one wave number $k = 2\pi$. The same domain and mesh as for the incompressible case are used. The boundary condition are now:

- walls: $\frac{\partial p}{\partial n} = 0$, with n the normal direction
- inflow: $p = 1$
- outflow: to ensure the outgoing wave with no reflection, a Perfectly Matched Layer (PML) is used [12].

The PML consists in artificially adding damping while the wave approaches the boundary. A new wave number is defined as

$$k' = k(1 + i\epsilon), \quad (12)$$

where ϵ is a small control parameter which is zero to describe normal propagation and non-zero (~ 0.1) to describe the damped propagation. The subsequent outflow condition is written:

$$\frac{\partial p}{\partial n} = -ik(1 + i\epsilon)p, \quad (13)$$

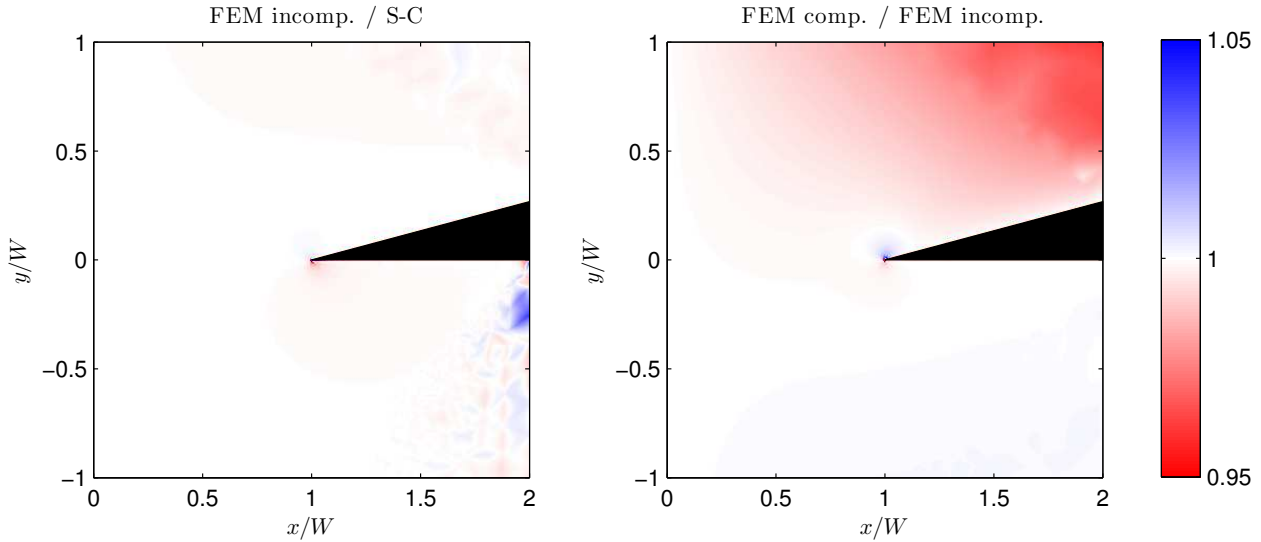


Figure 4. Ratio of the angle of the velocity field θ_i/θ_j , where $\theta = \arctan(v/u)$ and where the indices are relative to the methods (either Schwarz-Christoffel transformation or incompressible FEM or compressible FEM). Left: FEM incompressible over Schwarz-Christoffel. Right: FEM compressible over FEM incompressible.

corresponding to the damped wave propagation through the boundary of normal direction n . The acoustic velocity is then deduced from the pressure field and Euler's equation:

$$\begin{cases} u' = \frac{ik}{\rho_0 c_0} \frac{\partial p}{\partial x} \\ v' = \frac{ik}{\rho_0 c_0} \frac{\partial p}{\partial y} \end{cases}, \quad (14)$$

where ρ_0 is the air density and c_0 the speed of sound in the air.

3. COMPARISON OF THE METHODS

Since the complex potential and the Schwarz-Christoffel methods required a very basic geometry, the four previous methods are compared within the same (and ideal) configuration, i.e. with a sharp labium.

Figure 3 shows the streamlines (isovalue of the stream function ψ) around the sharp labium for the four methods. All the methods provide the same global trend of the flow around the labium. The complex potential does not account for the walls and the streamlines are not bended as it is the case for the other methods.

Every numerical method diverge while approaching the tip of the labium. Thus comparison is made impossible at this precise location. However, within the digit precision allowed by the computer, the power law of the divergence for the three numerical methods has been check to be as expected by the the complex potential. This point will be discussed later in section 4.

Rather than the absolute value of the velocity, the pertinent information is the direction of the velocity. This can be described by the angle θ that accounts for the ratio of the y-component over the x-component of the velocity through

$$\theta = \arctan \frac{v}{u}. \quad (15)$$

This scalar definition allows to compare the field in a two dimensional plot (see figure 4). The Schwarz-Christoffel

transformation and the incompressible FEM give almost the same results, at least near the labium. This gives support to the FEM method.

Then, the comparison between incompressible and compressible is made with the FEM method. The incompressibility is characterized by the Mach number $M = 4u_0/c$ and the Helmholtz number $He = W/\lambda = fW/c$. In both cases the inflow velocity $u_0 \approx 0.01\text{m/s}$ yields a Mach number $M \approx 10^{-4}$. The compressible case is computed with a "large" wavelength ($k = 2\pi$) yielding a Helmholtz number $He = 0.004$. For a soprano recorder, the Helmholtz number would remain under the value corresponding to the highest note (D7, 2350Hz): $He \approx 0.027$. The two methods show some little discrepancies in the upper area, i.e. the outward area. This can be due to the hypothesis made on the outflow condition in Eqs. (10) and (13) for the incompressible and compressible cases, respectively. However, this does not exclude that the incompressible outflow and the compressible radiation behave differently within the outward area. This is interpreted as the visible difference between incompressible and compressible flow.

Besides, it must not be forgotten that the flow is assumed incompressible since W is much smaller than the wavelength, but an oscillating flow is expected to occur on the streamline computed under this assumption.

4. APPLICATION TO A MORE REALISTIC CASE

The FEM method allows the previous and idealized case of the sharp labium to be extended to the more realistic case of a round labium. The previous configuration is modified by introducing a curvature R at the tip of the labium as sketched on figure 5. Results for this new configuration are discussed in the two following sections in which both parameters R and α are varied, respectively.

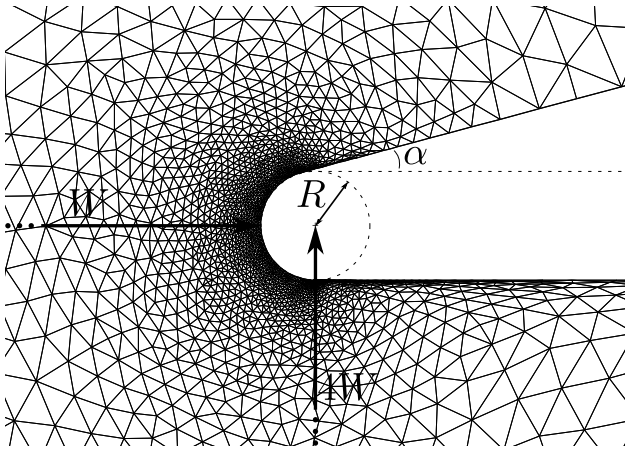


Figure 5. Modification of the tip of the labium to a rounded tip.

4.1 Sharpness of the labium

The radius R has been varied within a wide range of values from $R = W/1000$ to $R = W/10$, for one angle $\alpha = 15^\circ$. The divergence law of the velocity within the window is compared with the complex potential case (see Eq. (6)) on figure 6.

For all the value of R , the velocity shows the same trend according to three distinct areas: close to the wall ($x \lesssim W/2$), close to the labium ($x \gtrsim R$) and between these two areas. The middle area shows the same power law as expected by the complex potential method. When going from the wall to the middle area, the y -component of the velocity v goes from a non zero and constant value to the expected behaviour. When getting closer to the labium, the velocity stops increasing to reach a finite value: the velocity does no longer diverge and this effect starts at a distance $\sim R$ from the tip of the labium.

Besides stabilizing an unrealistic and diverging case, the

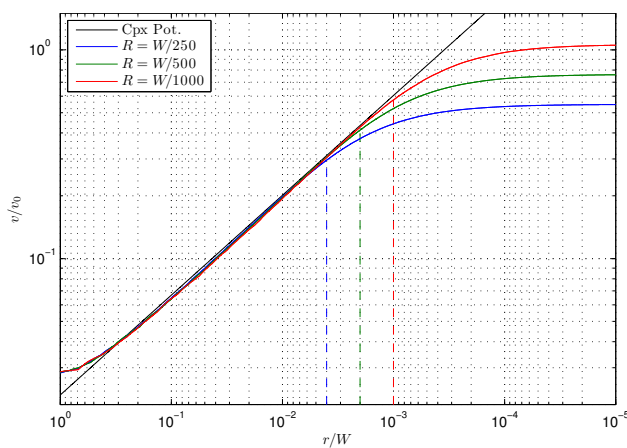


Figure 6. y -component of the velocity v in the window ($y = 0$) versus dimensionless radius r/W for $\alpha = 15^\circ$ and for different values of R . The radius r is defined as $r = W - x$. Note that the r axis is reversed in order to match to the orientation of the other figures. Vertical dashed lines correspond to the different radii.

curvature triggers a slower increase of the velocity while approaching the labium. The bigger the curvature R , the larger the distance at which the velocity stops increasing and the lower the amplitude of the velocity at an arbitrarily close distance to the labium.

4.2 Angle of the labium

The angle α has been varied within a wide range of values from $\alpha = 0^\circ$ to $\alpha = 60^\circ$, for one radius $R = W/500$. The divergence law of the velocity within the window is compared with the complex potential case (see Eq. (6)) on figure 7.

Results are similar to those discussed in the previous section in terms of the global trend according to the three specific areas. As expected, only the value of the divergence exponent n in Eq. (6) is modified by the angle of the labium: the slope of the velocity v in the $(\log r, \log v)$ plane depends on α only.

Thus, at a distance arbitrarily close to the labium, for a same inflow u_0 the y -component of the velocity v increases as the angle decreases.

5. DISCUSSION AND CONCLUSION

Different methods to study the acoustic flow around the labium of a recorder have been compared for one simple case. The use of incompressible flow methods is justified at low frequencies since the distance W of the window is much smaller than the acoustic wavelength. The Finite Element Method (FEM) is validated in comparison to the complex potential method, in the case of an incompressible flow. The assumption of having an incompressible flow within the window is checked using the FEM: compressible and incompressible FEM give almost the same results. Little discrepancies arise within the outward area. This is interpreted as an effect of the compressibility.

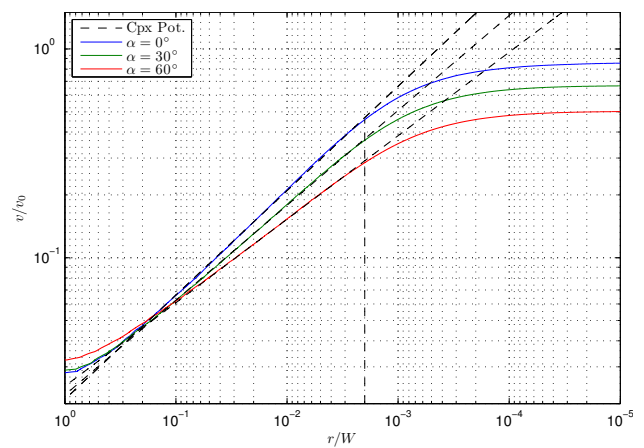


Figure 7. y -component of the velocity v in the window ($y = 0$) versus dimensionless radius r/W for $R = W/500$ and for different values of α . The radius r is defined as $r = W - x$. Note that the r axis is reversed in order to match to the orientation of the other figures. The vertical dashed line correspond to the radius $R = W/500$.

The FEM method presented in this paper is a little more useful than the previous Schwarz-Christoffel transformations made by other authors on the same issue, since it can be applied to more realistic configurations. However, the present study only provides solutions for the potential component of the flow and reaches its limit when the whole flow might be required. This is the case for aeroacoustic analogies, such as Lighthill's one, where the non potential component of the flow is interpreted as sources for the potential component. Besides, other phenomena are also not caught by the potential description: neglecting the viscosity is an other important limitation. Viscous effects are though dominant at the singularity of the potential flow, at the tip of the labium. When the gradient of the velocity increases, boundary layer might grow due to the viscosity and the (acoustic) flow might shed. This has been observed in flute-like configuration, for high amplitude of oscillation [4]. This is usually described as the formation of a free jet that occurs every half period [1, 13] and dissipates energy. Despite all these limitations, the study of the potential flow around the labium still provides usable results for more complex studies that would include both potential and non potential descriptions, and it provides some insights about the point discussed above.

The FEM confirms intuitive results about the growth of the velocity near the labium. When far enough from the wall, the velocity grows as expected for an ideal case. When close enough to the labium (at approximately one radius of curvature of the labium), the velocity ceases growing. It provides quantitative behaviours of the y-component of the velocity v with respect to both the sharpness and the angle of the labium: v increases with the sharpness and with a decrease of the angle. A higher y-component velocity is expected to trigger non-linear effects sooner. From there onwards, it may be possible to find a criteria based on other studies [14] to link the present linear description to non-linear phenomena. This may find application in reducing the trigger of this non-linear effect that is known to be a limiting factor in the growth of the amplitude of oscillation [4] and thus of the acoustic power.

These results come from a numerical computation. It would be interesting however to compare them to an analytical solution of the flow. The complex potential corresponding to the more realistic geometry (walls, labium with round edge) might be difficult to find. However, the present Schwarz-Christoffel transformation that already acknowledges for the walls can be adapted to localized round edges [15]. This would provide an analytical framework from which the results about the growth of the velocity near the edge should be confirmed.

The shape (angle and sharpness) of the labium has never been investigated through modeling. Dequand *et. al* proposed a *discrete-vortex* model that can include the orientation of the acoustic field near the labium. In such modeling, the sound production is ensured by the interaction of discrete vortices with the acoustic streamlines. It is common to consider the vortices close to the labium only: they have a greater contribution than far ones, since the acoustic velocity is greater near the tip of the labium. From the present

study, this assumption can be refined by considering vortices in an area whose characteristic length is of same order than the curvature radius of the labium. The *discrete-vortex* approach is a poor approximation of the flow so that an accurate estimation of the acoustic flow is an overkill when combining with these models. However, the combination would still provide a first tool to study the effect of the angle and/or the sharpness on the sound production.

6. REFERENCES

- [1] U. Ingard and H. Ising, "Acoustic Nonlinearity of an Orifice," *J. Acoust. Soc. Amer.*, vol. 42, no. 1, pp. 6–17, 1967.
- [2] M. S. Howe, "Contributions to the theory of aerodynamic sound, with application to excess jet noise and the theory of the flute," *Journal of Fluid Mechanics*, vol. 71, pp. 625–673, 9 1975.
- [3] —, "The dissipation of sound at an edge," *J. Sound Vib.*, vol. 70, pp. 407–411, 1980.
- [4] B. Fabre, A. Hirschberg, and A. P. J. Wijnands, "Vortex Shedding in Steady Oscillation of a Flue Organ Pipe," *Acust. Acta Acust.*, vol. 82, pp. 863 – 877, 1996.
- [5] P. A. Nelson, N. A. Halliwell, and P. E. Doak, "Fluid Dynamics of a Flow Excited Resonance, Part II: Flow Acoustic interaction," *J. Sound Vib.*, vol. 91, no. 3, pp. 375–402, 1983.
- [6] S. Dequand, J. F. H. Willems, M. Leroux, R. Vullings, M. Van Weert, C. Thieulot, and A. Hirschberg, "Simplified models of flue instruments : Influence of mouth geometry on the sound source," *J. Acoust. Soc. Amer.*, vol. 113, no. 3, pp. 1724–1735, 2003.
- [7] J. Darrozes and C. Francois, *Mecanique des Fluides Incompressibles*. Springer, 1982.
- [8] T. A. Driscoll, "Algorithm 756; a MATLAB toolbox for Schwarz-Christoffel mapping," *ACM Transactions on Mathematical Software*, vol. 22, pp. 168–186, Jun. 1996.
- [9] M. Verge, R. Caussé, B. Fabre, A. Hirschberg, A. Wijnands, and A. van Steenberg, "Jet oscillations and jet drive in recorder-like instruments," *Acta acustica*, vol. 2, no. 5, pp. 403–419, 1994.
- [10] F. Hecht, O. Pironneau, K. Ohtsuka, and A. L. Hyaric, <http://www.freefem.org/ff++>, 2013.
- [11] F. Hecht, "The mesh adapting software: bamg," *INRIA report*, 1998.
- [12] J.-P. Berenger, "A perfectly matched layer for the absorption of electromagnetic waves," *J. Computational Physics*, vol. 114, pp. 185–200, Oct. 1994.
- [13] J. H. M. Disselhorst and L. V. Wijngaarden, "Flow in the Exit of Open Pipes During Acoustic Resonance," *J. Fluid Mech.*, vol. 99, pp. 293–319, 1980.